STUDIES ON ANHYDRITE CEMENTATION IN GEOTHERMAL RESERVOIRS

H. Pape[1], C. Clauser[1], J. Iffland[2], J. Bartels[3], R. Wagner[1], M. Kühn[4]

[1] Aachen University of Technology (RWTH), Applied Geophysics, Germany
[2] LUNG Mecklenburg-Vorpommern, Germany
[3] Geothermie Neubrandenburg GmbH, Germany
[4] Technische Universität Hamburg-Harburg, Wasserwirtschaft und Wasserversorgung, Germany

Direct use of geothermal heat based on producing hot water in one borehole and injecting cool water in a second one requires an aquifer which meets the following minimum requirements: a thickness of 20 m, a permeability of 250 mD, and a temperature of 60 °C. The last condition corresponds roughly to a minimum depth of 1500 m. In northern Germany, a few sandstone formations meet these requirements, among them the Upper Keuper Rhaetian sandstone. In one particular borehole (Allermoehe 1, south of Hamburg) the Rhaetian aquifer was drilled at 3250 m with sufficient thickness and fluid temperature. The pore space, however, was cemented by anhydrite resulting in porosities as low as 2%. This motivated several coordinated research projects in order to investigate the conditions leading to this type of cementation.

Two main aquifers were drilled, the Contorta sandstone of the Middle Rhaeth and the Postera sandstone of the Lower Rhaeth. A classification of the rock type with respect to free fluid porosity, capillary bound porosity and clay bound porosity was based on a NMR log (CMR measured by Schlumberger). The Postera sandstone was cored from 3221.5 to 3259.6 m. In addition to the general core analysis (porosity, permeability, and pore radius distribution), special investigations on cores were performed by several groups. We studied 18 samples for several petrophysical properties. The comparison of the NMR porosity-log with the anhydrite volume content (Figure 1) shows that the section of sandstone with very low porosities (Pr 7, Pr 8, and Pr 10) experienced mainly chemical compaction by anhydrite cementation starting with an initial porosity of up to 27%. The anhydrite concentration was measured by chemical analysis of sulphur content combined with x-ray diffraction. For more information on pore structure depending on anhydrite cementation, induced polarization measurements were performed by F. Börner (Dresdner Grundwasserzentrum) and PFG-NMR (pulsed field gradient-nuclear magnetic resonance) measurements by J.

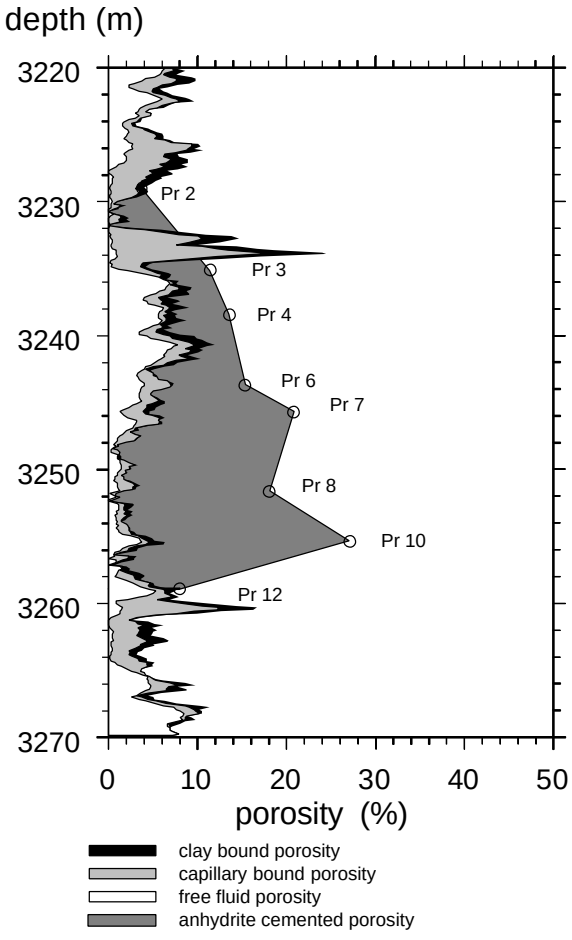

Fig. 1. NMR log of the Contorta sandstone in the well Hamburg-Allermoehe 1 (northwest Germany) and anhydrite cemented porosity measured on cores.

[1] h.pape@geophysik.rwth-aachen.de

back to contents

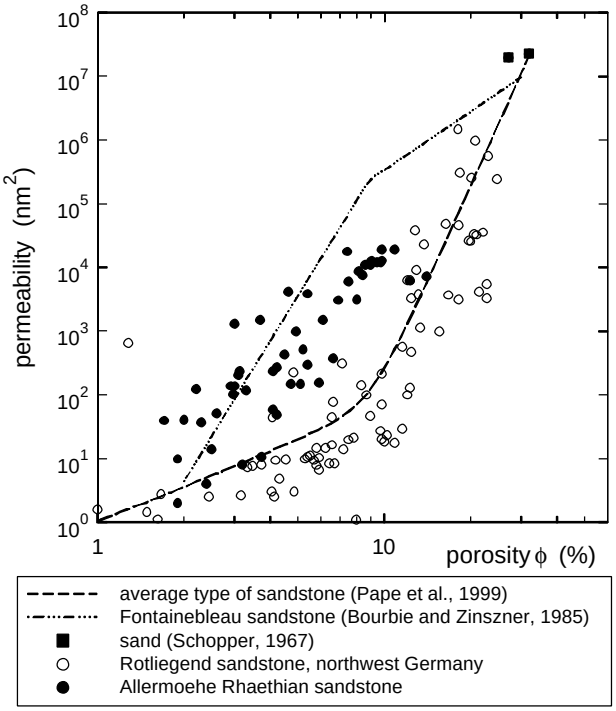

Fig. 2. Log-log plot of permeability versus porosity for sandstones of different diagenesis type. The average type is represented by data of Rotliegend sandstone of northwest Germany. Data of Rhaetian sandstone from Allermoehe span the field between the curve of Fontainebleau sandstone and average sandstone.

Tillich and M. Holz (University of Karlsruhe).

The diagenetic evolution of a sandstone formation is reflected by the permeability-porosity (k-ϕ) data in a log-log plot (Figure 2). According to Pape et al. (1999), data of average sandstones obey a concave curve, which can be expressed by

$$k = A\,\phi + B\,\phi^2 + C\,(10\,\phi)^{10}\,, \quad (1)$$

where the coefficients A, B, and C are proportional to the effective grain radius $(r_{grain})^2$. Equation 1 was derived under the assumption that a general parameter of pore structure, the fractal dimension D, remains constant with D = 2.36 (Pape et al., 1999, 2000). David et al. (1994) measured similar curves for various sandstones during mechanical compaction experiments. Diagenesis of sandstone starts with unconsolidated sand for which data are given by Schopper (1967).

In contrast, a convex curve was found by Bourbie and Zinszner (1985) for quartz cemented Fontainebleau sandstone expressed by

$$k = 303\,(100\phi)^{3.05} \quad (\mathrm{nm}^2) \quad \text{for } \phi > 0.08, \quad (2a)$$
$$k = 0.0275\,(100\phi)^{7.33}\,(\mathrm{nm}^2) \quad \text{for } \phi \le 0.08. \quad (2b)$$

Similar convex curves were found in pressure solution experiments with hot-pressed calcite (Bernabé et al., 1982) and from sintering of dry glass beads (Mok et al., 2000). In all these cases a smooth surface of the porous medium was maintained which corresponds to a fractal dimension close to the limiting value D = 2. Mok et al. (2000) modified these experiments by allowing metamorphic reactions under hydrothermal conditions which resulted in concave curves like the permeability-porosity relationship (Equation 1). Keehm et al. (2001) found both types of curves in pore scale numerical simulations of cementation depending on the pore filling mechanism: Preferential cementation at the grain contacts yielded a convex curve, while an inward shift at each point of the grain boundaries led to the curve of average sandstones.

Table 1. Petrophysical data of core samples from the Rhaeth of Allermoehe.

sample	porosity	anhydrite	ρ_{mtx}	S_{mtx}^{BET}	D	κq	phase	median pore radius	pore radius
		volume content						(mercury injection)	PFG-NMR
	%	%	g/cm^3	µm^{-1}	()	S/m 10^{-3}	mrad	µm	µm
Pr 2	3.73	0.00	2.66	3.56	2.39	1.73	-8.46	0.04	
Pr 12	14.00	0.00	2.63	0.58	2.26	5.48	-0.41	4.05	6.82
Pr 4	10.80	2.79	2.64	0.58	2.26	1.66	-0.90	4.72	10.14
Pr 6	8.89	6.46	2.66	0.94	2.30	3.29	-1.15	4.28	7.06
Pr 7	2.96	17.83	2.72	0.26	2.19	3.22	-0.16	0.36	7.28
Pr 8	3.13	14.96	2.71	0.18	2.15	1.99	-0.58	0.53	8.33
Pr 10	2.21	24.89	2.72	0.05	2.05	2.19	-0.34	0.46	11.28

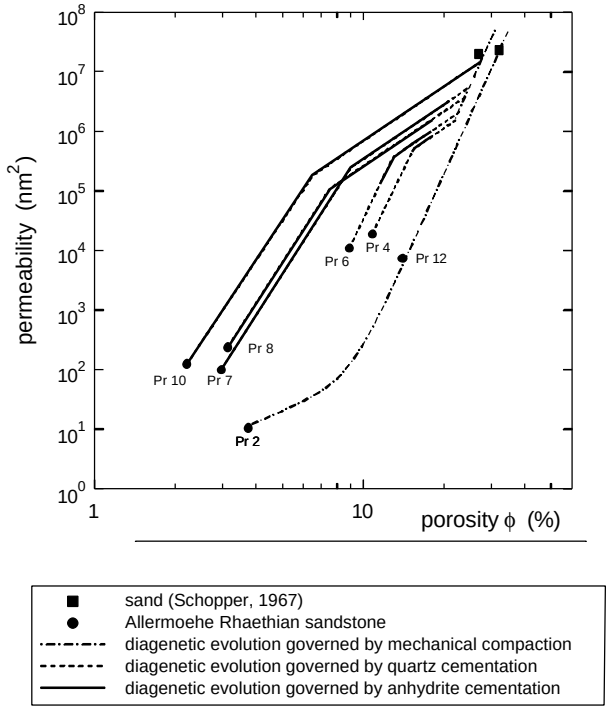

Fig. 3. Diagenetic evolution of different types of Allermoehe Rhaetian sandstone represented in a log-log plot of permeability versus porosity.

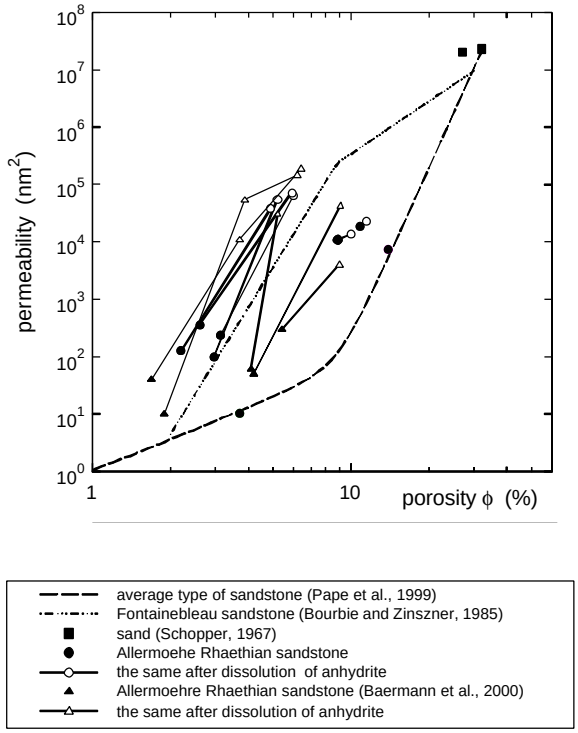

Fig. 4. Changes by dissolution of anhydrite in Allermoehe Rhaethian sandstone represented in a log-log plot of permeability versus porosity.

With respect to the permeability-porosity relationship, the studied Allermoehe Rhaethian sandstone samples clearly belong to different types of diagenesis (Figure 2). This could be proved by the petrophysical investigations (Table 1). In order to characterize the compaction mechanism of our samples, the fractal dimension *D* was calculated from the specific

surface normalized to matrix volume, which was measured on the one hand as $S_{mtx}(\lambda_1) = S_{mtx}^{BET}$ with high resolution by Nitrogen adsorption and which secondly was calculated with low resolution on the other hand as $S_{mtx}(\lambda_2) = 3/r_{grain}$ from:

$$S_{mtx}(\lambda_1) / S_{mtx}(\lambda_2) = (\lambda_1 / \lambda_2)^{2-D}, \qquad (3)$$

where the values $\lambda_1 = 0.001$ mm and $\lambda_2 = r_{grain}$ are the minimum resolved lengths of the two methods.

The samples of Table 1 are plotted into the permeability-porosity plot of Figure 3 assuming diagenetic paths according to their position with respect to the curve of average sandstones and the curve of quartz cemented Fontainebleau sandstone. The compaction by anhydrite cementation is represented by thick lines in Figure 3. Three groups of samples can be distinguished:

- Pr 2 and Pr 12 are not cemented and lay on the permeability-porosity curve of average sandstones. Pr 2 is a siltstone with large specific surface and large negative phase angle.
- Pr 4 and Pr 6 are cemented by anhydrite to a minor extend. They are probably quartz cemented.
- Pr 7, Pr 8, and Pr 10 are strongly cemented by anhydrite. This coincides with small fractal dimensions and small negative phase angles. The median pore radius, which is a measure of the radius of pore necks is reduced, while the radius of the pores themselves, calculated from PFG-NMR measurements, is the same as in the less cemented sandstones.

Anhydrite dissolved when the samples equilibrated with the saturating fluid for electrical measurements. At the end of these experiments, porosity and permeability were measured anew. The changes by anhydrite dissolution are shown in Figure 4 together with the results from flooding experiments by Baermann et al. (2000). Comparison of cementation (Figure 3) and dissolution (Figure 4) shows that the paths in the permeability-porosity diagram of the group of strongly cemented samples are the same, but in the opposite direction. No hysteresis arises from cementation and dissolution curves. This can be explained by the structural changes caused by the growth and solution of anhydrite crystals. They filled the pore space in optical continuity surrounding the quartz grains. At low porosities the cemented patches come into touch and percolation pathways are closed. Subsequent dissolution opens preferential pathways which leads to a steep increase of permeability.
In the less cemented samples, the initial change in permeability by dissolution of anhydrite is small. In this case the small and isolated patches of anhydrite cementation are small and isolated and don't restrict the percolation on a larger scale.
The study of permeability-porosity relationships depending on cementation is of interest for numerical simulations with coupled heat and fluid flow, chemical transport and geochemical reactions. It is planned to simulate different scenarios of anhydrite cementation on pore scale and on geological scale (Kühn et al., 2000).

ACKNOWLEDGEMENTS
The research reported in this paper was supported by the Deutsche Forschungsgesellschaft (DFG) under grant Cl 121/11-1 and by the German Federal Ministry for Education, Science, Research, and Technology (BMBF) under grant 032 70 95.

REFERENCES
Baermann, A., Kröger, J., and Zarth, M., "Anhydritzemente im Rhätsandstein Hamburgs – Röntgen- und kernspintomographische Untersuchungen und Lösungsversuche", *Z. angew. Geol*., (2000) **46**, 3, 144-152.
Bernabé, Y., Brace, W. F., and Evans, E., "Permeability, porosity and pore geometry of hot-pressed calcite", *Mech. Mater.*, (1982) **1**, 173-183.
Bourbie, T., and Zinszner, B., "Hydraulic and acoustic properties as a function of porosity in Fontainebleau sandstone", *J. geophys. Res*., (1985) **90,** B13, 11524-11532.
David, C., Wong, T., Zhu, W., and Zhang, J., "Laboratory measurements of compaction-induced permeability change in porous rocks: implications for the generation and maintenance of pore pressure excess in the crust", *Pure Appl. Geophys*., (1994) **143**, 1/2/3, 425-456.
Keehm, Y., Mukerji, T., Nur, A., "Computational rock physics at the pore scale: Transport properties and diagenesis in realistic pore geometries", The Leading Edge, (2001) 2, 180-183.
Kühn, M., Bartels J. , Pape, H., Schneider, W., and Clauser, C., " Modeling chemical brine-rock interaction in geothermal reservoirs", in: *Water Rock Interactions* (eds. Stober, I., Bucher, K.) Kluwer, Dortrecht in press.
Mok, U., Bernabé, Y., and Evans, B., "Permeability, porosity and pore geometry of chemically altered porous silica glass", submitted to *JGR*, (2000).
Pape, H., Clauser, C., & Iffland, J., "Permeability prediction for reservoir sandstones based on fractal pore space geometry", *Geophysics,* (1999) **64**, 5, 1447-1460.
Pape, H., Clauser, C., and Iffland, J., "Permeability-porosity relationship in sandstone based on fractal pore space geometry", *Pure appl. geophys.*, (2000) **157**, 603-619.
Schopper, J. R. "Experimentelle Methoden und eine Apparatur zur Untersuchung der Beziehungen zwischen hydraulischen und elektrischen Eigenschaften loser und künstlich verfestigter poröser Medien", *Geophys. Prospecting*, (1967), **15,** 4, 651-701.

back to contents